Reducing false-positive SARS-CoV-2 diagnoses using long-range RT-qPCR

Aartjan J.W. te Velthuis[1,2,*], Dovile Juozapaite[3], Charlotte V. Rigby[1,2,4], Ingrida Olendraite[1,3], Pankaj Mathur[5], Kalyan Dhanorkar[5], Vishalraj Hulle[5], Tejes Shah[6], Vijeta Jadhao[6], Shraven Mutha[6], Hamid Jalal[4], Vikram Gopal[5*]

[1] University of Cambridge, Department of Pathology, Addenbrooke's Hospital, Cambridge CB2 2QQ, United Kingdom.
[2] Lewis Thomas Laboratory, Department of Molecular Biology, University of Princeton, Princeton, 08540 NJ, United States.
[3] Vilnius University Hospital Santaros Klinikos, Hematology, Oncology and Transfusion Medicine Center, Santariskiu st. 2, 08661 Vilnius, Lithuania
[4] Public Health England, Addenbrooke's Hospital, Cambridge CB2 2QQ, United Kingdom.
[5] Pune Instrumentation Pvt. Ltd., PCNTDA, Bhosari, Pune, 411026, India.
[6] Krsnaa Diagnostics Ltd, Chinchwad, Pune, 411033, India

* Address correspondence to: aj.te.velthuis@princeton.edu; VGopal@umich.edu

Key words: SARS-CoV-2, influenza A virus, RT-qPCR, UVC inactivation, long-range

Abstract

Quantitative polymerase chain reaction (qPCR) is a sensitive molecular method for the detection of genetic material and regarded as the gold-standard for diagnostic testing. To detect respiratory RNA virus infections, a reverse transcription (RT) step is implemented to create cDNA molecules that can serve as template in the qPCR step. However, positive RT-qPCR results can be found long after patient recovery, in part because the RT-qPCR can detect residual viral RNA genome fragments. To minimize the detection of such fragments, we here modified the RT-qPCR assay by replacing the routinely used random hexamers with an oligonucleotide that binds to the 3′ end of the viral genome. We demonstrate that this method allows us to distinguish between infectious and non-infectious samples. Moreover, in clinical samples obtained over 15 days after the onset of symptoms, we observe that the modified RT-qPCR protocol yields significantly fewer positive results compared to a commercial RT-qPCR test. No significantly different results were found compared to the commercial test when SARS-CoV-2 clinical samples were tested within 5 days of the onset of symptoms, suggesting that the modification has a similar sensitivity for detecting infectious viral RNA. Overall, these findings may help differentiate between false-positive, persistently positive, and reinfection cases in COVID-19 patients.

Importance

Various molecular tests can be used to detect RNA virus infections. The RT-qPCR test is currently regarded as the gold-standard, but its sensitivity to residual viral RNA genome fragments can lead to “incorrectly-positive” RT-qPCR results. Technically, these results are different from false-positive RT-qPCR results, which can be generated due to in vitro cross-reactivity or contaminations. However, the detection of RNA fragments leads to similar incorrect conclusions about the presence of infectious virus long after a patient has recovered from a viral infection and thus false-positive diagnoses. These false-positive diagnoses affect patient hospitalization and treatment, including transplantations. We here modified a commercial RT-qPCR kit to make it less sensitive to residual viral RNA genome fragments, reducing the likelihood for false-positive results in recovered COVID-19 patients. The method may improve test-to-release protocols, expand the tools available for clinical testing, and help reduce hospital encumbrance.

Introduction

Respiratory RNA viruses, such as influenza and coronaviruses, are important human pathogens that have substantial impact on our healthcare systems and economy (1, 2). The detection of viral RNA infections in symptomatic and asymptomatic patients is essential to prevent respiratory virus spread, monitor patient recovery, and perform triage in hospitals. Currently, reverse transcription quantitative polymerase chain reaction (RT-qPCR)-based tests are considered the gold-standard for the detection of viral RNA in clinical samples.

RT-qPCR assays consist of two steps: cDNA synthesis and PCR amplification (Fig. 1). Typically, random hexamers are used for cDNA synthesis. These primers can bind anywhere in the viral genome and even to remnants of viral RNA genomes, allowing them to contribute to the RT-qPCR signal (Fig. 1A), making it more complicated to distinguish between infectious and non-infectious viral genomes. Indeed, the contribution of genome fragments to the RT-qPCR signal has been proposed as explanation for the persistence of positive signals after the recovery from Coronavirus disease 2019 (COVID-19) (3-5).

To minimize the synthesis of cDNA molecules from viral RNA genome fragments, we here used an oligonucleotide that binds to the 3′ end of the viral genome and is subsequently extended into a long (or long-range) cDNA product. When the viral genome contains breaks, cDNA synthesis will stop at the breakpoints, leading to the production of short cDNA products that cannot serve as qPCR template (Fig. 1). In line with previous influenza A virus studies (6, 7), we find that the long-range RT-qPCR method facilitates the differential detection of infectious and non-infectious virus, and untreated or UVC exposed viral RNA. Moreover, the RT-qPCR method yields significantly fewer positive results in clinical samples obtained after COVID-19 recovery, but not in samples obtained within the first 5 days of the onset of COVID-19 symptoms. These findings suggest that the long-range RT-qPCR method can be used to reduce the number of false-positive COVID-19 diagnoses.

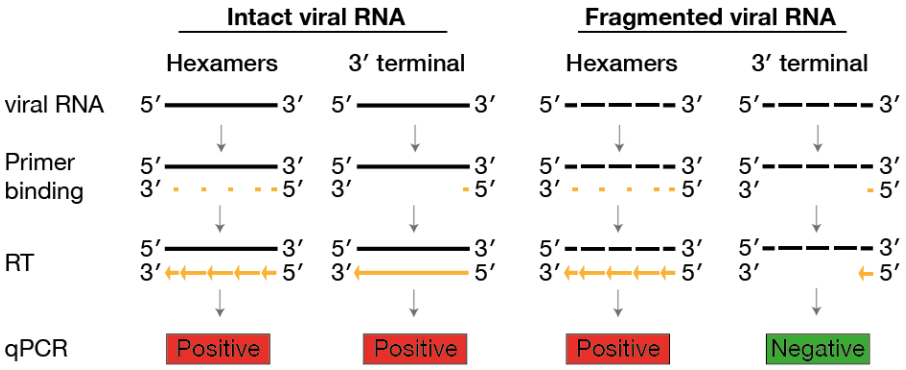

Figure 1. Schematic of differential RT-qPCR detection of intact or fragmented viral RNA using an RT step that is dependent on random hexamers or a primer binding to the 3′ terminus of the viral RNA.

Methods

Ethics nasopharyngeal swabs

Nasopharyngeal swabs were obtained by Krsnaa Diagnostics Ltd. (KDL) for experimental use. Our use of these swabs was reviewed by the National Accreditation Board for testing and calibration Laboratories (NABL) and the authorized signatories of KDL for the Late. Jayabai Nanasaheb Sutar Hospital, and approved on 22 June 2021. KDL is accredited by the NABL with ISO 15189:2012 compliance and approved by ICMR, with ICMR code KDPLP. RNA extracted from nasopharyngeal swabs for the time-course analysis of SARS-CoV-2 infections were obtained from Vilnius Santaros Klinikos Biobank (Vilnius, Lithuania). The investigation was approved by Vilnius Regional Bioethics Committee (approval number 2021/5-1342-818).

Viruses and cells

HEK 293T, Vero-E6 and MDCK cells were originally sourced from ATCC. Influenza A/WSN/33 (H1N1) virus was produced by transfecting a 12-plasmid rescue system into HEK 293T cells (8). After two days, the P0 virus was amplified on MDCK cells in Minimal Essential Medium (MEM; Gibco) containing 0.5% fetal bovine serum (FBS; Sigma) at 37 °C and 5% CO_2. P1 and P2 viruses were aliquoted and stored at -70 °C. SARS-CoV-2 Bavpat-1 was grown on Vero-E6 cells in Dulbecco's Minimal Essential Medium (DMEM; Gibco) containing 0.5% FBS at 37 °C and 5% CO_2. Viral RNA was extracted using Trizol (Invitrogen) as described previously (9).

UVC chamber and exposure

For UVC exposure, we used a Suraxa® UVC chamber (Pune Instrumentation Private Limited (PIPL)). The unit contained four 254 nm UVC light tubes (Philips) whose output could be adjusted manually and measured using a UV light power meter placed in the center of the unit. The setting used were 11, 32, 43 or 54 W. Samples were placed in a polystyrene well (TRP product number 92012) and positioned, without lid, on the bottom rack in the middle of the UVC chamber. UVC exposures were subsequently performed as indicated in the results section and figures. After UVC exposure, virus was eluted using 275 µl PBS/0.05% Tween-80 (10) and transferred to 1.5 ml tubes for plaque assays.

Plaque assays

Plaque assays were performed as described previously (10). Briefly, samples were serially diluted in MEM containing 0.5% FBS. Two hundred µl of diluted virus was next added to confluent MDCK cells and incubated for 1 hour 37 °C. After virus adsorption to the MDCK cells, the inoculum was removed and replaced with 2 ml MEM/agarose overlay (MEM, 0.5% FBS, 1% agarose). Plaques were grown for 2 days at 37 °C and then fixed

with 4% paraformaldehyde in PBS. Plaques were counter-stained with 0.01% crystal violet in water and washed with tap water before analysis.

RT-qPCR analysis of influenza virus RNA levels

Viral RNA was extracted from 50 µl of elution material using Trizol (Invitrogen) as described previously (9). Extracted RNA was resuspended in 10 µl water. Next, 1 µl of viral RNA was used for reverse transcription with universal influenza 3′ primer TUMI 12G or random hexamers (Thermo Fisher) and superscript III (Invitrogen). qPCR was performed using primers specific for the NA segment (11) and Brilliant III Master Mix with high Rox (Agilent) on a Step-One plus qPCR machine.

RT-qPCR analysis of UVC exposed SARS-CoV-2 RNA samples

Viral RNA was extracted from 50 µl of elution material using Trizol (Invitrogen) as described previously (9). Extracted RNA was resuspended in 10 µl water. Next, 1 µl of viral RNA was used for reverse transcription with oligo-dT_{20} (Thermo Fisher) or random hexamers and superscript III. qPCR was performed using previously described primers specific for the ORF1ab or N coding regions (12). The qPCR was run and analyzed on a QuantStudio 5 or Step-One plus qPCR machine according to the manufacturer's instructions.

RT-qPCR analysis of time course samples

Viral RNA was extracted using the MagMAX Viral/Pathogen Nucleic Acid Isolation Kit (Thermo Fisher). Next, 4 µl of RNA was mixed with 1 µl of 50 µM oligo-dT_{20} (Thermo Fisher) and 6.4 µl of water. The primer/RNA mix was incubated for 2-3 min at 95 °C and immediately placed on ice afterwards. cDNA produced using Maxima H minus reverse transcriptase (Thermo Fisher) at 50 °C for 1 hour according to the manufacturer's instructions. qPCR analysis was performed by adding 5 µl of cDNA to a TaqPath qPCR reaction (Thermo Fisher). The qPCR was started with a 2 min 95 °C denaturation step to inactivate the RT enzyme in the TaqPath kit. This was then followed by 40 cycles of 3 sec 95 °C and 30 seconds at 60 °C. The reactions were analyzed on a QuantStudio 5 qPCR machine.

Statistics

For statistical testing, we used one-way ANOVA and multiple corrections. Statistical testing was performed using GraphPad Prism 9.0.

Role of the funding sources

The funders of the study had no role in study design, data collection, data analysis, or writing of the manuscript.

Results

Detection of infectious and non-infectious influenza A virus

To investigate the ability of RT-qPCR methods to distinguish between active and inactivated RNA viruses, we used ultraviolet C (UVC) at 254 nm to inactivate influenza A virus strain A/WSN/1933 (H1N1). UVC can create cross-links or breaks in nucleic acid strands and inactivate influenza A virus (6, 13, 14) and SARS-CoV-2 (15-20). Following optimization and calibration of our instrument (Fig. S1A), we exposed 25 µl 10^6 pfu/ml influenza A virus to 54 W of UVC for 5 to 60 seconds. The exposed virus was subsequently serially diluted to determine the virus titer by plaque assay and found to be completely inactivated after 60 seconds (Fig. 2A). Viral RNA was next extracted and generated cDNA using random hexamers or a universal influenza A virus primer capable of binding to the 3′ end of the viral genome. cDNA levels were subsequently analyzed using primer sets specific for the influenza A virus M or NA segment (Fig. S1B and 2A, respectively). qPCR signals obtained with the 3′ end cDNA showed an increase in Ct value that was strongly correlated with the virus titer and length of UVC exposure (Fig. 2A). No effect of UVC was observed on the viral nucleoprotein level, which forms ribonucleoprotein complexes with the viral RNA (21) (Fig. S1B). By contrast, the qPCR signal obtained with the random hexamers showed a smaller change in Ct value (Fig. 2A). Together these results suggest that a long-range RT-qPCR protocol that uses a primer that binds to the 3′ end of the viral genome during the cDNA synthesis reaction provides the best estimate of the infectious viral titer.

SARS-CoV-2 RNA detection

To investigate if a 3′ RT primer can differentiate between UVC-exposed and unexposed SARS-CoV-2 RNA, SARS-CoV-2 RNA from infected cells was exposed to 54 W of UVC for 0 to 120 sec. Next, RT reactions were performed using random hexamers or an oligo-dT_{20} primer capable of binding to the 3′ polyA-tail of the SARS-CoV-2 RNA genome. Subsequent qPCR analysis using CDC-recommended primer sets targeting the N and ORF1ab coding regions showed a clear change in the Ct value as function of the exposure time for the 3′ samples amplified with both primer sets (Fig. S2), but a relatively limited change in Ct value for the random hexamer samples with both primer sets (Fig. S2). We next exposed COVID-19 clinical samples to UVC and detected the intact viral RNA genome levels using random hexamer or oligo-dT_{20} for the cDNA synthesis. As shown in Fig. 2B, we observed a significant difference between the UVC exposed and unexposed samples using the oligo-dT_{20} method, but not using random hexamers.

Finally, we investigated if the two RT-qPCR methods yielded different results over the course of a SARS-CoV-2 infection. To this end, we analyzed clinical samples obtained within the first 5 days of the onset of symptoms (i.e., when SARS-CoV-2 infected patients are typically infectious) and samples obtained at least 15 days after the onset of symptoms (i.e., when most patients have recovered). As shown in Fig. 2C and Table S1,

we observed no significant difference between the two RT-qPCR methods for the COVID-19 samples taken withing 5 days of the onset of symptoms, suggesting they are equally efficient at detecting infectious viral RNA levels in clinical samples. However, a significant difference was observed in samples obtained more than 15 days after the onset of symptoms (Fig. 2C), with most long-range RT-qPCR reactions producing no detectable signals (Table S2).

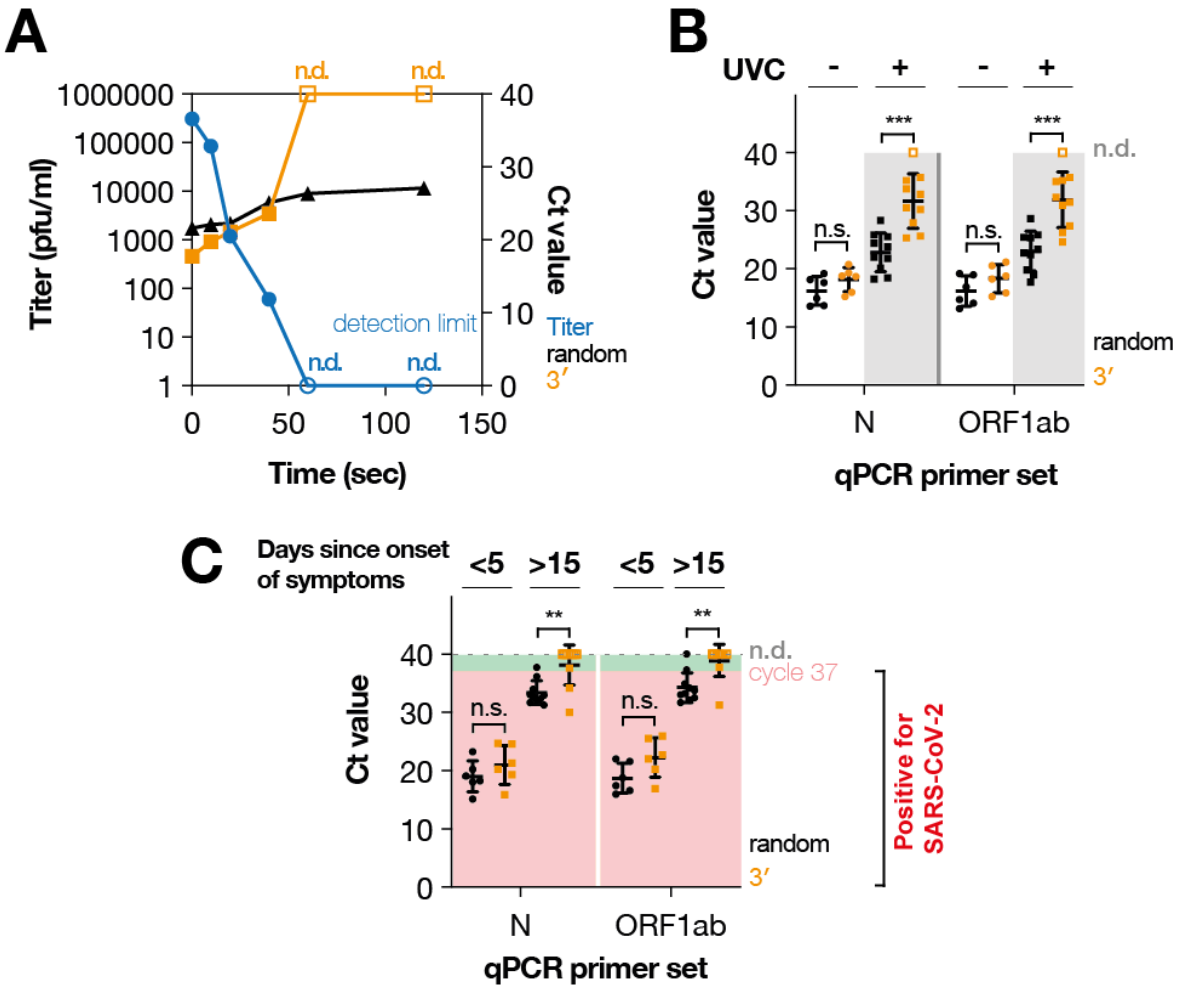

Figure 2. Differential detection of intact and fragmented viral RNA using RT-qPCR. (**A**) Relation between UVC exposure at 54 W, the influenza A virus A/WSN/1933 titer, and the qPCR signal following RT reactions with random hexamers or a universal influenza A virus primer capable of binding to the 3′ terminus of each of the eight viral RNA segments. qPCR was performed using primers specific for the NA segment. Plaque assay results that were not detectable (n.d.) are indicated. RT-qPCR signals that were not detectable are shown as Ct = 40 on graph. (**B**) RT-qPCR of COVID-19 clinical samples following 0 or 120 seconds of 54W of UVC exposure. (**C**) RT-qPCR of COVID-19 clinical samples obtained within 5 days of the onset of clinical symptoms or after 15 days following the onset of clinical symptoms. RT-qPCR signals that were not detectable are shown as Ct = 40 on graph. Significance was tested using one-way ANOVA with multiple corrections. Not significant (n.s.), $p < 0.01$ (**), $p < 0.001$ (***).

Discussion

We here used primers that bind to the 3′ terminus of the influenza A virus genome segments, or SARS-CoV-2 genome and subgenomic mRNAs to eliminate the detection of inactivated viral RNA by RT-qPCR. Our results confirm previous observations with influenza A viruses (6, 7) that this long-range RT-qPCR protocol more closely matches the measurements of infectious virus levels using plaque assays than RT-qPCR methods primed with random hexamers. We demonstrate that the long-range RT-qPCR shows significantly reduced positive SARS-CoV-2 results in nasopharyngeal samples taken more than 15 days after the onset of symptoms. Moreover, within 5 days of the onset of symptoms, we observed no significant differences, suggesting that the two methods do not have an inherent different sensitivity for detection infectious COVID-19 cases. Previous research has shown that COVID-19 patients can test positive for SARS-CoV-2 long after recovery (5). Our method can be used to reduce these false-positive RT-qPCR tests, and distinguish between incorrectly-positive cases and reinfections.

Author contributions

Conceived study: AJWtV, VG. Designed and performed experiments: AJWtV, CR, DJ, IO. Contributed reagents and equipment: PM, KD, VH, TS, VJ, SM, VG. Reviewed and performed data analysis: AJWtV, DJ, CR, IO, VG. Wrote manuscript draft: AJWtV. Contributed to manuscript finalization: AJWtV, DJ, CR, IO, PM, KD, VH, TS, VJ, SM, HJ, VG.

Data sharing

Ct values of COVID-19 clinical samples are provided in supplemental tables. Reagents and other data are available upon request.

Declaration of interests

All other authors declare no competing interests.

Acknowledgments

AJWtV is supported by joint Wellcome Trust and Royal Society grant 206579/Z/17/Z. CR is supported by PhD training grant G107570 from Public Health England.

References

1. J. K. Taubenberger, D. M. Morens, Pandemic influenza--including a risk assessment of H5N1. *Rev Sci Tech* **28**, 187-202 (2009).
2. R. A. Medina, A. Garcia-Sastre, Influenza A viruses: new research developments. *Nat Rev Microbiol* **9**, 590-603 (2011).
3. S. Ikegami *et al.*, Persistence of SARS-CoV-2 nasopharyngeal swab PCR positivity in COVID-19 convalescent plasma donors. *Transfusion* **60**, 2962-2968 (2020).
4. C. D. Mack *et al.*, SARS-CoV-2 Transmission Risk Among National Basketball Association Players, Staff, and Vendors Exposed to Individuals With Positive Test Results After COVID-19 Recovery During the 2020 Regular and Postseason. *JAMA Intern Med* **181**, 960-966 (2021).
5. L. Lan *et al.*, Positive RT-PCR Test Results in Patients Recovered From COVID-19. *JAMA* **323**, 1502-1503 (2020).
6. Y. Nakaya, T. Fukuda, H. Ashiba, M. Yasuura, M. Fujimaki, Quick assessment of influenza a virus infectivity with a long-range reverse-transcription quantitative polymerase chain reaction assay. *BMC Infect Dis* **20**, 585 (2020).
7. D. Li, A. De Keuckelaere, M. Uyttendaele, Application of long-range and binding reverse transcription-quantitative PCR to indicate the viral integrities of noroviruses. *Appl Environ Microbiol* **80**, 6473-6479 (2014).
8. E. Fodor *et al.*, Rescue of Influenza A Virus from Recombinant DNA. *Journal of Virology* **73**, 9679-9682 (1999).
9. A. J. W. Te Velthuis, J. S. Long, W. S. Barclay, Assays to Measure the Activity of Influenza Virus Polymerase. *Methods Mol Biol* **1836**, 343-374 (2018).
10. V. Gopal *et al.*, Zinc-Embedded Polyamide Fabrics Inactivate SARS-CoV-2 and Influenza A Virus. *ACS Appl Mater Interfaces* **13**, 30317-30325 (2021).
11. A. J. W. Te Velthuis *et al.*, Mini viral RNAs act as innate immune agonists during influenza virus infection. *Nat Microbiol* **3**, 1234-1242 (2018).
12. C. Reusken *et al.*, Laboratory readiness and response for novel coronavirus (2019-nCoV) in expert laboratories in 30 EU/EEA countries, January 2020. *Euro Surveill* **25** (2020).
13. J. J. McDevitt, S. N. Rudnick, L. J. Radonovich, Aerosol susceptibility of influenza virus to UV-C light. *Appl Environ Microbiol* **78**, 1666-1669 (2012).
14. E. I. Budowsky, S. E. Bresler, E. A. Friedman, N. V. Zheleznova, Principles of selective inactivation of viral genome. I. UV-induced inactivation of influenza virus. *Arch Virol* **68**, 239-247 (1981).
15. C. W. Lo *et al.*, UVC disinfects SARS-CoV-2 by induction of viral genome damage without apparent effects on viral morphology and proteins. *Sci Rep* **11**, 13804 (2021).
16. A. Gardner, S. Ghosh, M. Dunowska, G. Brightwell, Virucidal Efficacy of Blue LED and Far-UVC Light Disinfection against Feline Infectious Peritonitis Virus as a Model for SARS-CoV-2. *Viruses* **13** (2021).
17. M. Bormann *et al.*, Disinfection of SARS-CoV-2 Contaminated Surfaces of Personal Items with UVC-LED Disinfection Boxes. *Viruses* **13** (2021).
18. W. K. Jung, K. T. Park, K. S. Lyoo, S. J. Park, Y. H. Park, Demonstration of Antiviral Activity of far-UVC Microplasma Lamp Irradiation Against SARS-CoV-2. *Clin Lab* **67** (2021).
19. Y. Qiao *et al.*, Greater than 3-Log Reduction in Viable Coronavirus Aerosol Concentration in Ducted Ultraviolet-C (UV-C) Systems. *Environ Sci Technol* **55**, 4174-4182 (2021).

20. Y. Gerchman, H. Mamane, N. Friedman, M. Mandelboim, UV-LED disinfection of Coronavirus: Wavelength effect. *J Photochem Photobiol B* **212**, 112044 (2020).
21. A. J. te Velthuis, J. M. Grimes, E. Fodor, Structural insights into RNA polymerases of negative-sense RNA viruses. *Nat Rev Microbiol*, 1-16 (2021).